Roylance, D., P. Chammas, J. Ting, H. Chi, and B. Scott

# Numerical Modeling Of Fabric Impact

Procedings of the National Meeting of the American Society of Mechanical Engineers (ASME)
San Francisco, October 1995

## ABSTRACT

A numerical code has been developed to model the complex behavior of woven fabric panels subjected to ballistic impact. The code has the ability to model multiple-layer fabric panels, multiple projectile geometries, and fabric imperfections such as yarn slippage at cross-overs and also at clamps. A discussion of the numerical methodology is presented, along with the results of numerical simulations of impact on single and multiple-layer fabrics, with and without resin impregnation.

## METHOD OF ANALYSIS

The numerical algorithms used in our impact code are basically finite difference approximations of simple physical laws, as will be outlined below. This approach, sometimes called "direct analysis" in light of its simplicity, was first suggested by Mehta and Davids (1966) and their coworkers for a variety of dynamics simulations, and was adapted by Roylance and coworkers (1973, 1981) to the study of impact on woven textile panels. The codes based on the method appear to be well suited for flexible armor analysis and design: it is relatively simple to understand and implement, yet seems to capture the important physics of the impact event with good accuracy.

The general nature of our impact algorithm will be outlined here briefly; the reader is referred to a report by Roylance and Houghton (1989) for further detail. In our simulations, the fabric reinforcement panel is idealized as an assemblage of pin-jointed, massless fiber elements. The fabric crossover points, or "nodes", are assigned a mass that makes the areal density of the idealized mesh equal to that of the panel being simulated. The density of crossovers in the numerical model need not necessarily be the same as that in the actual panel. The code is currently restricted to zero-obliquity impact of a square-symmetric panel, though these limitations could be relaxed at the expense of code complexity.

The initial projectile velocity is imposed on the node at the impact point, which causes a strain to develop in the adjacent elements. The tension resulting from this strain is computed from a material "constitutive" (stress-strain) relation, and this tension is used to calculate an acceleration of the neighboring nodes. The computer proceeds outward from the impact point, successively using a momentum-impulse balance, a strain-displacement condition, and a constitutive equation to compute for each element the current values of tension, strain, velocity, position, and such ancillary but important quantities as strain energy and kinetic energy. At the end of these calculations, a new projectile velocity is computed from the tensions exerted on the projectile by the fibers, and the process is repeated for a new increment of time.

The masses of the fiber elements are taken to be lumped at the nodal crossover points, so that each node incorporates half the mass of the four fiber elements meeting at that node:

$$m_n = \frac{1}{2}\zeta\rho\Delta l \qquad (1)$$

The parameter $\rho$ is the lineal fiber density, read into the FORTRAN variable **`denyrn`** in textile units of denier (mass in grams of a 9,000 m length of yarn). The parameter $\Delta l$ is the length of the fiber element connecting the nodes, and $\zeta$ is a numerical factor associated with the crimping and weave of the fabric structure. The crimping factor $\zeta$ (named **`crimp`** in the computer code) is in turn computed by dividing the actual mass of the experimental fabric panel by that which would have been obtained simply by multiplying the lengths of the various fiber elements by their density.

This crimping factor provides a means of simulating multiple-layer fabrics while retaining an essentially single-layer algorithm; the user provides a value for the actual multiple-layer panel mass, and the appropriate mass adjustment is incorporated into the crimping factor. The crimping factor allows the use of numerical meshes coarser than the actual weave, since it serves to make the areal densities of the actual and simulated fabrics the same.

The tensions in the fiber elements meeting at the node cause an acceleration of the nodal mass, and this effect is described by a straightforward application of Newton's Second Law:

$$\mathbf{T} = m_n \frac{\Delta \mathbf{V}}{\Delta t} \qquad (2)$$

Here $\Delta\mathbf{V}$ is the change in velocity of the node in a time increment $\Delta t$, where boldface type is used to indicate vector quantities. Then knowing $\Delta\mathbf{V}$, an updated nodal velocity can be computed from the value in the previous time increment. The tensile force **T** has five contributing components, one from each of the four fiber elements meeting at the node, and one more from a fictitious "backup" spring of stiffness $k_b$ attached to the node and oriented perpendicularly to the fabric panel.

The backup spring provides a force in the direction opposite the projectile velocity, and in earlier versions of the code was intended to simulate the effect of the human torso in resisting the displacement of fabric armor during impact. In more recent work, we have explored

using the spring to simulate the effect of the impregnating polymer matrix in a composite material on the ballistic resistance of the composite.

Once new nodal velocities have been computed from Newton's law as described above, the coordinates representing nodal positions can be updated for the current time increment. The strain ε in each fiber element can then be computed by using the new nodal coordinates to compare the current fiber length with the original undeformed length. The fiber tension can be related to the strain by the material's dynamic constitutive relationship, and the code has a number of material models available. For the case of a simple elastic fiber of modulus *E*, tension is calculated from the strain by the simple form of Hooke's law:

$$T = E\,\varepsilon \qquad (3)$$

(The code uses units of gm/den for both *T* and *E*.) Of course, a number of constitutive relations beyond simple Hookean elasticity are possible, and versions of the code have implemented models for linear and nonlinear elasticity and viscoelasticity. However, in many of our impact simulations we have no experimental indications that these more elaborate models are necessary, and we commonly assume a linear elastic model.

At each time increment, the algorithm "marches" outward from the impact point, sequentially updating the values for position, strain, tension, and velocity of the fabric nodes. After indexing the node counters from the impact point to the upper-right node in the half-quadrant, the projectile velocity $V_p$ is updated and the loop over the fabric nodes is begun again. The projectile velocity is corrected by means of a momentum balance between the projectile deceleration and the tensions acting on the projectile by the four fiber elements connected to the impact point, and also the decelerating force provided by the backup spring.

The fiber element length $\Delta l$ is user-specified, by selecting the number of nodes **`jt`** spanning the distance from the impact point to the edge of the fabric. However, the time increment $\Delta t$ cannot be specified arbitrarily, since the ratio of the length and time increments must satisfy a numerical stability criterion:

$$\frac{\Delta l}{\Delta t} < c_f \qquad (4)$$

where $c_f$ is the wavespeed in the fabric. This wavespeed is less than the well-known value $c = \sqrt{(E/\rho)}$ expected for single fibers, since the crossovers act effectively to double the mass density sensed by the propagating wave. This line of reasoning, which is admittedly conjectural and in need of further study, leads to $c_f = c\sqrt{2}$. To permit alternative relations, the time increment is computed by the code as:

$$\Delta t = \frac{\Delta l}{c_f} = \frac{\Delta l}{\alpha\sqrt{E/\rho}} \qquad (5)$$

where usually we take $\alpha = \sqrt{2}$.

The numerical method requires appropriate initial and boundary conditions in order to proceed with the computation. The initial condition is that all nodal points are at rest except that the initial projectile velocity is imposed at the center of the panel, i.e. $V_{1,1} = V_p$. The boundaries of the fabric are assumed to be rigidly clamped during impact, thus $V_{x=L/2} = 0$. The code also has the capability of relaxing this condition to permit both fiber-fiber and clamp slippage.

## NUMERICAL RESULTS

### Simulation of ballistic impact on single-layer fabrics

As the code runs, it spools numerical values for nodal positions and velocity, along with fiber tension, strain, and energy to output files that can be imported into auxiliary for further manipulation or plotting as desired. Figure 1 below shows typical data generated by the code, in this case the strain profiles along the fiber passing through the impact point at various times after impact.

In some cases, it is preferable to see a more global display of panel response, even at the expense of detail. For instance, it is possible to capture the displacement and strain fields for a given time after impact, and plot them in "four" dimensions. Such a 4-d graph in shown in Figure 2, where the *x*-*y*-*z* positions of the nodes are plotted as a surface graph. (The *z* position, out of the fabric plane, is magnified.) The strain is then added to this graph as color (displayed as shades of gray here). Such a display makes it easy to see, for instance, that the strain propagates will ahead of the "transverse wave" behind which the fabric experiences a *z*-direction displacement.

The algorithm is terminated when the projectile has been brought to zero velocity or when a failure criterion is satisfied somewhere in the fabric. The code can be set to begin a new impact simulation at a reduced starting velocity $V_s$,, so that the response of a panel over a range of impact velocities can be plotted. In both experimental and theoretical work on armor, a plot of the starting velocity $V_s$ versus the residual velocity $V_r$ is a useful measure of the armor's ballistic resistance. In particular, the value of $V_s$ at which $V_r$ becomes zero approximates $V_{50}$, the experimental impact velocity at which there is a 50% probability of penetration.

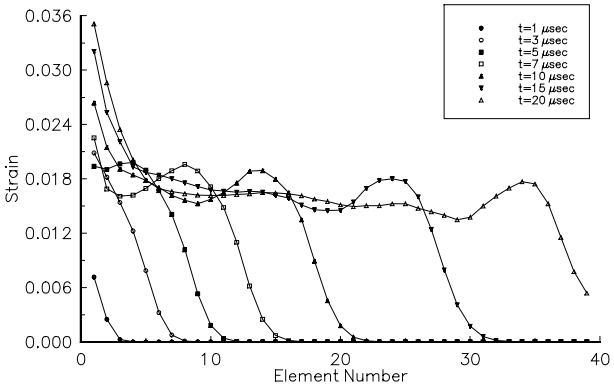


Figure 1: Distribution of tensile strain along fiber passing through impact point at various times after impact. (Single layer panel of 1500 denier Kevlar 29 fabric, backup spring stiffness $k_b$ = 0, projectile mass 17 grains.)

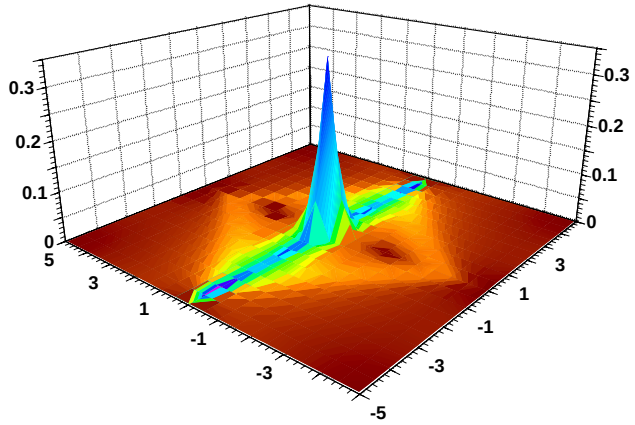


Figure 2: Full-field map of displacement ($z$ - direction) and strain (color) during fabric impact. Here the strain in the fibers running from lower left to upper right are plotted.

In its PC implementation, the code employs a dynamic graphical display that shows the full-field strain throughout a fabric panel, as well as the strain along the fiber passing through the impact point during code execution. Since a typical impact event takes place in fractions of a millisecond, it is extremely difficult for an experimentalist to instrument or measure the strains and displacements in a fabric panel. At the expense of some code execution speed, this display provides the ability to visualize the dynamic behavior of the panel.

The computer display contains three sections, as shown in Figure 3. The major portion of the screen displays the uni-directional strain in each model fiber segment in the upper right quadrant of the panel. The display uses color to indicate the strain magnitude, which unfortunately cannot be seen in the figure. On the actual display, there are a total of 16 different colors arranged in a spectrum with blue representing near zero strain and red representing strain near the breaking strength of the material. In the lower right corner, the strain along the model fiber passing through the impact point is plotted vs. distance along the fiber. Above the plot, there is a display of current code parameters such as the projectile velocity, the impact event time, and the maximum value and position of the uni-directional strain throughout the fabric.

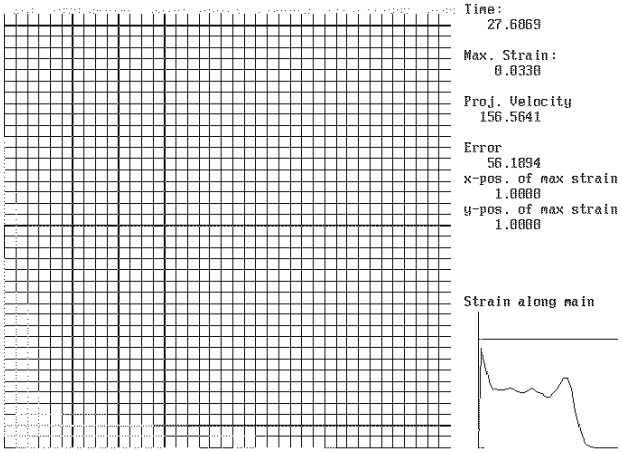


Figure 3: Sample graphic display during fabric impact simulation.

## Simulation of resin stiffening by means of "backup springs."

As stated earlier, our simplest model assumes only a single layer of fabric, and simulates the effect of multiple layers by increasing the numerical density of the fabric. Figure 4 shows computed $V_s - V_r$ data obtained using this model with a numerical areal density comparable to three layers of fabric (code variable **`lyr`** =3). Here the stiffness of the backup spring stiffness $k_b$ was varied parametrically to assess its influence.

The following table lists the $V_{50}$ for these simulations, given by the value $V_s$ at which $V_r$ becomes zero, for the various values of the backup spring stiffness.

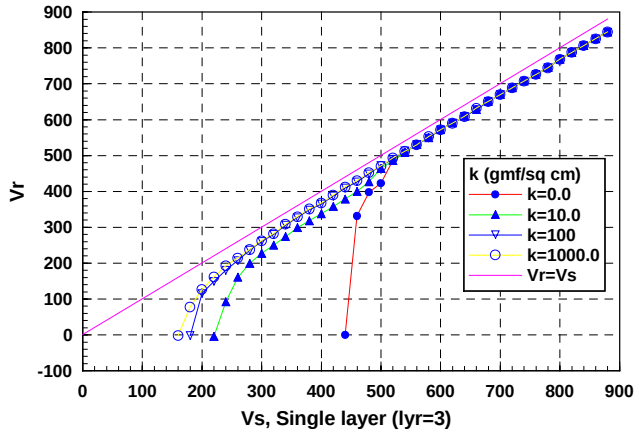


Figure 4: Plot of $V_s$ vs. $V_r$ using the single layer model for different values of the backup spring and simulating (by adjusting the numerical areal density) a 3 layer fabric. Each data symbol represents the result of a single impact simulation.

| $k_b$, gmf/cm$^2$ | $V_{50}$, m/s |
|---|---|
| 0 | 440 |
| 10 | 220 |
| 102 | 190 |
| 103 | 160 |

As seen here, the ballistic resistance decreases with increasing values $k_b$. For instance, increasing the spring stiffness from 0 to 100 gmf/cm$^2$ reduced the $V_{50}$ by 57%. Note that these spring stiffnesses are artificial, being small compared with typical polymer moduli: 1000 gmf/cm$^2$ is 98.0 kPa, or 14.2 psi.

This reduction in $V_{50}$ as $k_b$ increases appears to be related to the tendency of the backup spring to impede *z*-direction movement of the fabric; this movement imparts a transverse impact to fibers other than those passing through the impact point, and is a significant mechanism for energy distribution.

As expected, the ballistic resistance is increased ($V_{50}$ increases) as more layers are added. Figure 5 shows *Vs- Vr* results obtained by varying the FORTRAN variable **`lyr`** to simulate fabrics of 3, 5, and 10 layers, and the table following lists the $V_{50}$ values.

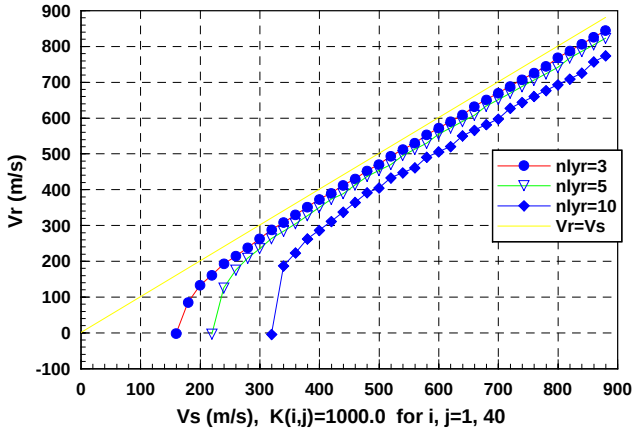


Figure 5: Plot of $V_s$ vs. $V_r$ using the single layer model for different number of layers and for backup spring stiffness $k_b$ =1000 gmf/cm$^2$.

In these simulations the backup spring stiffness was $k_b$ =1000.0 gmf/cm$^2$. Increasing the number of layers from 3 to 5 increased the $V_{50}$ by 24 % and increasing the number of layers from 3 to 10 increased the $V_{50}$ by 50%.

## Fiber Slippage at Crossovers

The code has also been modified to simulate fiber slippage, since examination of actual fabrics reveals what appears to be substantial fiber slippage. This is true especially of the fibers passing through the impact point. In previous versions of the code, the fiber elements were modeled as being perfectly pinned at their connecting nodes. The extent of slippage in actual fabrics probably depends on many different factors, to include the tightness of the fabric weave, the yarn friction coefficients, and moisture. Further experimental work is needed in this area.

To simulate the effect of slippage several lines of code have been added which compute the net normal and in-plane tensions at a node. The code computes the maximum amount of in-plane tension due to friction using two components. The first component, which is constant and given by the parameter **`sfrict`** with textile units of grams force/yarn denier (gmf/den), represents the friction due to the construction of the weave. The second component is equivalent to the dynamic friction due to the normal forces during impact. The code computes the dynamic friction by multiplying the normal force by a non-dimensional friction factor, **`sfric1`**, and adds this result to sfrict .

Several numeric experiments have been performed to assess the effectiveness of the code. Simulations were used to generate plots of residual velocity $V_r$ vs. initial striking velocity $V_S$ for 20.3 cm square panels of aramid fabrics, with 1.1 g (17 grain) projectiles. A model mesh size of 40 x 40 for one quadrant of the fabric panels was used for every set of analyses. The code has the ability to model projectiles with either circular or square impacting faces, although the coarse mesh used in these experiments did not allow a differentiation between the two projectile shapes. Both single and multiple layer fabrics were simulated.

First, a single layer of 1000 denier Kevlar 29 was studied for ballistic response using three different nodal slip conditions: **`sfrict`**=100, 500, 1000 gmf/den. Fiber-fiber friction rises as **`sfrict`** increases, presumably correlating with the tightness of the weave

| **`lyr`** | $V_{50}$, m/s |
|---|---|
| 3 | 160 |
| 5 | 220 |
| 10 | 320 |

as well. Results are shown in Figure 6 as plots of the residual velocity, $V_r$ vs. striking velocity $V_s$. The figure also shows experimental data provided by Cunniff (1992), taken from tests of a single panel of Kevlar 29 using a circular aperture plate 0.203 m in diameter to clamp the panel.

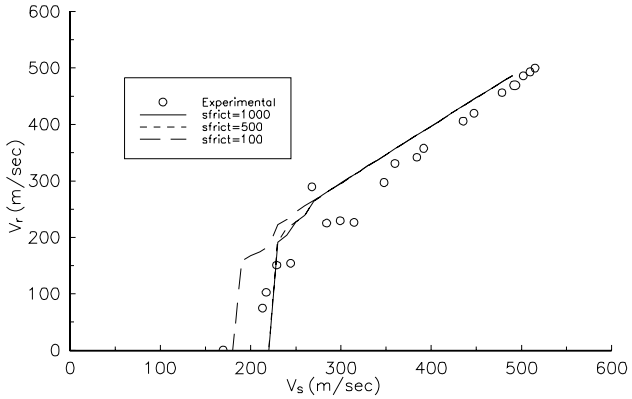


Figure 6 - Plot of Vs vs. Vr for a 203 mm (8 inch) single-layer panel of 1000 denier Kevlar 29 fabric modeled with a mesh size of 40x40 using three different slippage conditions.

The numerical results shown in Figure 6 indicate that the ballistic resistance as indicated by the computed $V_{50}$ value appears to decrease with a decrease in **`sfrict`**. The fabric panels with **`sfrict`** = 1000 and 500 gmf/den have a $V_{50}$ approximately 230 m/sec, while for the panel with **`sfrict`** = 100 gmf/den $V_{50}$ is only 180 m/sec. The general trend of these results agree with those from both Prosser (1985) and Cunniff (1992), who found that increasing yarn slippage at the impact point decreases performance.

## Multiple Layer Extension

The code has also been modified to simulate multiple layer fabrics. Previous versions of the code simulated the behavior of multiple layer fabrics by multiplying the effective modulus and weight of the fabric. The current version treats each layer as an autonomous system linked only at the points which are in contact; the initial separation of the layers is an adjustable parameter. The nodes in each layer are free to slide in-plane, but when they move out-of-plane, the code checks to see if there is contact between layers. If there is contact, the code computes the effective slowdown due to the resulting inelastic collision. After contact between layers occurs, the code computes the node displacement by summing the forces due to all of the fiber segments in contact.

To illustrate this aspect of code operation, results are shown in Figure 7 from a ballistic impact event for a 9-layer panel of 1500 denier Kevlar 29, 20.3 cm square. Here the instantaneous out-of-plane positions of nodes along the fibers passing through the impact point are plotted vs. the distance from the impact point. Initially, the projectile is only in contact with one layer. The code then projects the position of the projectile and determines which layers are affected. As shown in Figure 3, all 9 layers are quickly brought into contact at the impact point, but the number of contacting layers drops quickly as a function of distance. At the next set of nodes, there are only 4 layers in contact, and at the set of nodes beyond that, the only active layer is the layer in contact with the projectile.

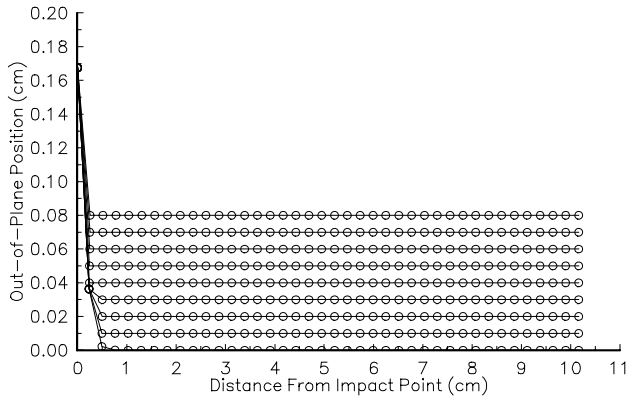

Figure 7 - Plot of out-of-plane positions along the main load bearing fiber for a 9-layer panel of 1500 denier Kevlar 29.

A set of numerical simulations was performed to assess the ability of the code to model multiple layer fabrics. One set of five panels was modeled with a spacing of 1.0 mm between layers, with this spacing chosen to reflect approximately the thickness of one single layer of fabric. The panels were all analyzed for their ballistic limits, and the resulting plots of $V_r$ vs. $V_s$ are shown in Figure 8. These results show that $V_{50}$ appears to be a nearly linear function of the number of layers. The slope of the curve gives an indication of the performance gained from increasing the number of layers and as a result, the areal density.

## CONCLUSIONS

The impact code provides a means of obtaining insight into the mechanics of fabric response during ballistic impact. It is fast and convenient to use, permitting use as a design tool for fabric ballistic protection devices.

We feel the model studies have shown that the backup-spring concept is a promising method for simulating ballistic impact in composite laminates, and that the single-layer model is sufficient for early design work. The springs definitely provide a measure of stiffness to the model fabric layer much as would be expected from an impregnating resin matrix. The resulting code is able to display both final fail-or-pass impact predictions, such as the $V_{50}$ value, and also transient information such as the distribution of strain or strain energy at various times after impact.

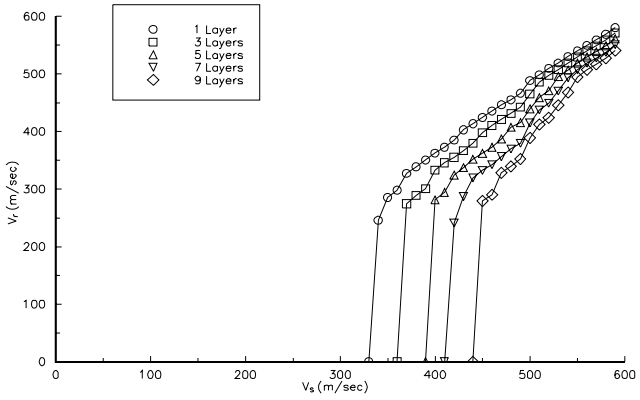


Figure 8 - Plot of Vr vs. Vs from simulations of a panel made from layers of 1500 denier aramid cloth with a gap of 1.0 mm between layers.

The backup spring array has a dramatic effect on the ballistic resistance of the fabric, generally predicting reduced ballistic resistance as the stiffness is increased if all nodal springs have the same stiffness. However, this was not necessarily true if the springs at positions away from the impact point are allowed to have lesser stiffness than that at the impact point itself.

As expected, increasing the numerical areal density of the fabric in the single-layer model to simulate the effect of having multiple fabric layers predicts an increase in the ballistic resistance of the fabric. Of course, this modeling approach ignores layer-layer interactions such as interlayer sliding.

Independent experimental data on typical material properties will be very useful in assessing the code predictions and to help tune some other input parameters that the model requires. This is especially true of the backup spring stiffnesses, which were too arbitrarily selected in this report.

In extending these studies, we feel it might be very effective to put some viscous behavior in the spring to simulate resin damping. It might also be fruitful to develop a more general force-field type of concept in place of the spring. This could simulate in-plane sliding as well as transverse motions of the fabric nodes.

## REFERENCES

Cunniff, P., 1992, "An Analysis of the System Effects in Woven Fabrics Under Ballistic Impact," *Textile Res. J.*, Vol. 62, pp. 495-509.

Mehta, P. and Davids, N., 1966, "A Direct Numerical Analysis Method for Cylindrical and Spherical Elastic Waves," *AIAA Journal*, Vol. 4, pp. 112-117.

Prosser, R.A., Aug. 1985, "The Penetration of Nylon Ballistic Panels by Fragment Simulating Projectiles, Part II Mechanics of Penetration," US Army Natick Research, Development and Engineering Center, Natick, MA, Technical Report TR-85/027L.

Roylance, D.K., A.F. Wilde, and G.C. Tocci, 1973, "Ballistic Impact of Textile Structures," Textile Research Journal, Vol. 43, pp. 34-41.

Roylance, D., and Wang, S.S., 1981, "Influence of Fiber Properties on Ballistic Penetration of Textile Panels," *Fiber Science and Technology*, Vol. 14, pp. 183-190.

Roylance, D., and Houghton, W. Aug. 1989, Improved Flexible Armor Design, First Phase Final Report, Contract DAAK60-87-R-0042, US Army Natick RD&E Center,.